

Novel Method of Separating Probe and Wire Bond Regions Without Increasing Die Size

Lois Yong, Tu Anh Tran, Stephen Lee, Bill Williams*, Jody Ross

Motorola Semiconductor Products Sector
Final Manufacturing Technology Center
7700 W. Parmer Lane
Austin, TX 78729

Lois.Yong@motorola.com, Tu.Anh.Tran@motorola.com, Stephen.chuchung.Lee@motorola.com,
RA2410@email.sps.mot.com

*Motorola Semiconductor Products Sector
Final Manufacturing Technology Center
1300 North Alma School Road
Chandler, AZ 85224
Bill.M.Williams@motorola.com

Abstract

The drive for enhanced electrical performance and reduced silicon area has triggered significant changes in wafer fabrication, wafer level testing, and packaging technologies. In the wafer fab, copper is quickly replacing aluminum as the interconnect metal of choice for technologies 0.13 μ m and below. To overcome the difficulty of wire bonding onto readily oxidized copper bond pads, capping copper bond pads with aluminum has been the industry standard remetallization for wire bonding for copper technology. In terms of wafer level testing and packaging, the resulting fine pitch geometry has created challenges for both cantilever probe and wire bond processes. Pad damage due to probe marks has been shown to cause "non-sticks" and "lifted bonds" at wire bonding. The wire bond yield loss due to pad damage is aggravated for fine pitch since increasingly smaller bonded ball diameters are formed on top of the same damage area caused by the probe mark. Wire Bond parameter optimization can minimize wire bond yield loss but cannot eliminate the problem. One logical solution is to lengthen the bond pad to create separate regions for probing and wire bonding. However, this method can result in a larger die size. This paper will reveal a unique bond pad structure that provides separate regions but yet results in no impact to the existing die size. This bond pad structure utilizes the aluminum cap layer to create a longer bond pad without changing the size of the underlying copper last metal, resulting in no impact to the existing die size. Evaluations were conducted on 0.13 μ m CMOS technology, with cantilever probing and wire bonding on 52 μ m bond pad size. Failure analysis and test methods to detect failures will be discussed. Designs of experiments for probing and wire bonding processes, characterization studies, and reliability results will be presented.

Key words: Copper, Probe, Probe Mark, Wire Bond, Aluminum cap, Fine Pitch, Bond Pad

Introduction

Copper is quickly replacing aluminum as the interconnect metal of choice for CMOS technologies 0.13 μ m and below. Cantilever probe technology has long been the most widely

used and cost effective method of conducting wafer level testing. Correspondingly, for packaging, wire bonding is the dominant means of interconnection between the silicon chip and the package. The ever-present drive for miniaturization of electronic products demands the need for silicon shrinks and smaller bond pad geometries. Copper interconnects, small bond pad sizes, and fine pitches between the pads present increasing challenges for both cantilever probing and wire bonding.

One of the primary issues is the interaction between the probe mark and the wire bond. The probe mark is the indentation left on the bond pad due to contact between the cantilever needle and the bond pad. For closely spaced and small bond pads, it has become increasingly difficult to control the size, location, and consistency of the probe mark. This creates significant damage on the bond pad, which results in difficulty of forming a bond during wire bonding. The resulting failure modes are "non-stick" during wire bonding, and "lifted bond" resulting in "low ball shear strength" during the ball shear test.

In order to utilize existing infrastructure and to overcome the difficulty of probing and wire bonding directly onto a copper bond pad, aluminum has been used to "cap" the copper bond pad^{1,2}. One of the concerns with this pad structure is the possibility of the probe mark scrubbing through and penetrating the aluminum and exposing the underlying copper. The exposed copper oxidizes, further exacerbating the difficulty of wire bonding onto the bond pad.

Common probe solutions to the issues described above have been focused on creating a smaller and more shallow probe mark. A typical strategy to make a smaller probe mark is to reduce the probe needle tip diameter. In some cases, 0.8mil and 0.6mil tips have been used. Small probe needles pose both fabrication and maintenance challenges. Many probe card suppliers have difficulties in controlling the size, location, and durability of these small probe needles. The life of the probe needle reduces dramatically as the diameter decreases. In addition, the need for special needle manufacturing processes and/or materials increases the cost of probe cards. These issues are amplified for high I/O devices where probe needles are configured in multiple tiers. Some

devices having 400 – 500 bond pads require 3 or 4 tiers of needles on a single probe card. On top of this, many devices require wafer level testing multiple times, on multiple die simultaneously and at elevated temperatures.

To minimize the depth of the probe mark and lessen copper exposure, a conventional method is to reduce the force exerted by the probe needle onto the bond pads. This is achieved by manufacturing the probe card at a lower spring force, and by reducing the overdrive during the probe process itself. However, in order to obtain valid wafer level test results, it is necessary to achieve good contact between the needle and the bond pad. Reducing the probe needle force may result in unstable test results.

To tackle the issues from the wire bond side, wire bond parameters such as ultrasonic power and bond force are adjusted. For larger bond pads, the bonded ball diameter can be increased so that the ratio of the ball bond to the probe mark is larger. This provides a higher percentage of “undamaged” aluminum pad for the bond to be created. However, with small bond pads, the damage on the bond pad caused by the probe mark is often too severe to be successfully wire bonded, even when the bonding parameters are fully optimized.

Solution – Bond Pad Structure

The solution to eliminate issues due to the interaction between the probe mark and the wire bond is to create separate regions on the bond pad for probing and wire bonding. With separate regions, the probe process can be optimized to maintain the lowest contact resistance with the bond pad without limiting the probe mark size to facilitate good wire bonding. Thus, the only constraint on probe mark size is the bond pad size. With a separate wire bond region, a clean, untouched bond pad is then available for wire bonding. This is crucial for wire bonding on small bond pads.

Figure 1 shows an illustration of a conventional bond pad with a shared probe and wire bond location. In Figure 2, a bond pad with separate probe and wire bond regions is shown.

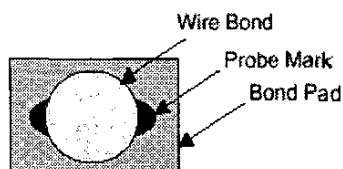


Figure 1: Conventional Bond Pad with Shared Probe and Wire Bond Location

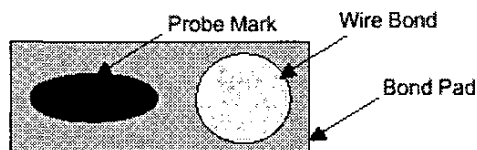


Figure 2: Bond Pad with Separate Probe and Wire Bond Regions

Figure 3 shows a cross-sectional illustration of a standard copper bond pad with an aluminum cap. To create two regions on a single bond pad, the bond pad must be lengthened. Since the aluminum cap is lengthened, the copper

bond pad is lengthened accordingly, thus creating a larger die size. This increases the overall cost of the device.

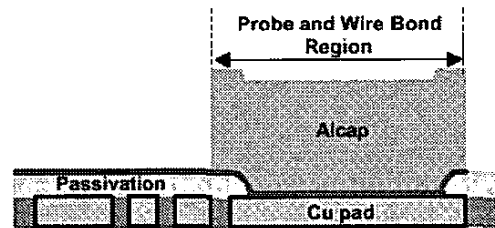


Figure 3: Cross-section of Standard Aluminum Cap Bond Pad

In Figure 4, a method of creating separate probe and wire bond regions without increasing the die size is presented. On an aluminum capped copper bond pad, the aluminum is extended over the passivation region beyond the underlying copper bond pad. Since the copper bond pad size remains the same, this pad structure allows for a longer bond pad with no impact to the size of the die. Furthermore, no additional wafer processing costs are incurred, since the aluminum and barrier layers are blanket sputtered on the entire wafer and etched to define the features.

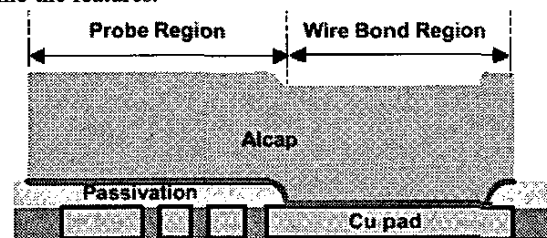


Figure 4: Cross-section of New Bond Pad with Separate Probe and Wire Bond Regions without Increasing Die Size

Preliminary Considerations

Theoretical calculations and simulations were conducted to determine the viability of using this bond pad structure.

Adhesion: Previous data^{1,2} had shown good adhesion between the copper-passivation-barrier-aluminum interfaces.

Contact Force: An estimate of the force per unit area exerted during probing and wire bonding was made. Typical values associated with probe forces are as follows:

| | |
|--------------------|-------------------------|
| Probe needle force | = 0.8g/mil of overdrive |
| Overdrive | = 50µm |
| Tip | = 0.8 mil |

$$ProbeForce = 0.8g / milOD \times 50\mu mOD \times \frac{1}{\pi(0.8mil^2/4)} = 3.13g / mil^2$$

Although a direct comparison cannot be made due to the different nature of the forces, this force is relatively low when compared to forces exerted during wire bonding. Admittedly, wire bond forces are difficult to estimate. However, typical values during wire bonding, without considering ultrasonic energy, are approximated as follows:

| | |
|----------------------|--------|
| Bonded Ball Diameter | = 38µm |
| Impact Force | = 29g |

$$\text{WireBondForce} = 29g \times \frac{1}{\pi \left(\frac{38\mu\text{m}^2}{4} \right)} = 16.5g / \text{mil}^2$$

Electrical Simulation: An electrical simulation was conducted to determine the capacitance effects of the additional aluminum metal. Simulation details will not be presented in this paper. The results indicated a negligible increase in capacitance as a result of the new bond pad structure.

Thermal Simulation: Likewise, there was no impact on thermal performance of the die or package associated with the increase in aluminum bond pad area.

Discussions in this paper will focus on the key experiments and evaluations conducted to ensure manufacturability and reliability of wafers containing the new bond pad structure. For clarity, the new bond pad structure will be referred to as POP (Probe Over Passivation).

Experimental Approach

The test vehicle used in this study was fabricated at 0.13 μm CMOS copper technology. The aluminum cap layer of the test vehicle was re-designed to extend the aluminum cap above the passivation and thus elongate the aluminum caps of bond pads such that a separate probe region was created on the passivation. The experiment was conducted in three parts:

- Probe performance comparison between standard location and POP location
- Wire bond yield, and
- Package reliability stress testing

a) Probe Performance Comparison between Standard Probe Location and POP Location

The overall purpose of the probe experiments is (1) to establish at the minimum requirement probe yield equivalency between the standard probe location and POP probe location; (2) to ensure no passivation cracking or copper metal damage underneath the POP probe marks across a range of probe process conditions; and (3) to establish new POP probe card specifications and probe process window that takes advantage of no interaction with wire bonding.

The cross-section and top-down views of the POP pad structure implemented on the test vehicle is shown in Figure 5. The standard probe location is the traditional location on which probe and wire bond are performed, whereas the POP probe location is the separate probe region above the passivation and away from the wire bond region. Since the POP pad was designed on all 178 bond pads, the probe performance can be compared between the standard probe location and POP location within each bond pad of the device.

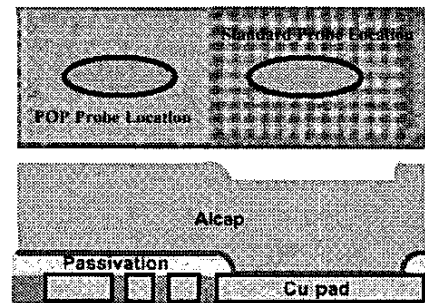


Figure 5: Standard and POP Probe Locations

Table 1 shows the three probe cards that were evaluated. All probe cards were fabricated with 0.8 mil needle tip diameter.

Table 1: Probe Cards Used in Evaluations

| Probe Card | Description |
|------------|--|
| Baseline | Baseline probe card targeting the <u>standard</u> probe location |
| POP Light | POP probe card targeting the POP probe locations and designed at the <u>same spring force</u> as the baseline probe card |
| POP Heavy | POP probe card targeting the <u>POP</u> probe location and designed at a <u>heavier spring force</u> |

The spring force designed for the baseline probe card and POP light probe card was optimized so as to provide a balance between low contact resistance during probing and minimal pad damage required for wire bonding. Since probing on the POP location eliminates the interaction between probe mark damage and wire bondability, the POP card with heavier spring force was evaluated to obtain the lowest contact resistance with no damage to the underlying passivation layer. This advantage can potentially widen the probe manufacturing window in terms of heavier contact force for lower contact resistance and less re-probe is needed.

A four-cell experiment presented in Table 2 was planned to provide the direct comparison of probe performance between the baseline probe card and the two POP probe cards. One wafer was used in each cell of the experiment. To exercise the operating range of the probe cards, two probe overdrive settings were used - a nominal overdrive setting and a heavy overdrive setting which is 20% higher than the nominal setting. On each wafer, all 2118 dice were probed at the standard location using the baseline probe card, then probed again at the POP location using the POP probe card at the probe conditions defined for each cell. To further understand the extent of passivation damage under POP locations due to multiple probe passes, the number of probe passes varied from 1, 2, 3 and 4 double-touch passes (i.e. 2, 4, 6 and 8 touches) across each wafer. Figure 6 depicts an example of the wafer map instruction for Cell 1 of the probe experiment.

Table 2: POP Probe Experiment Matrix

| | | Probe Card Type | | | Cell |
|-------------------------|---------|-----------------|-----------|-----------|------|
| | | Baseline | POP Light | POP Heavy | |
| Probe Overdrive Setting | Nominal | X | X | | 1 |
| | Heavy | X | X | | 2 |
| | Nominal | X | | X | 3 |
| | Heavy | X | | X | 4 |

Three types of responses were collected and compared on each of the four wafers: (1) electrical yield during probing, (2) mechanical characterization of probe mark (X- and Y-dimensions and depth measurement), and (3) inspection for passivation cracking and copper line disturbance underneath the POP locations.

Two methods used to inspect for passivation cracking or copper line disturbance are a chemical etching method and FIB inspection through the probe marks. The chemical etching method is a two-step process, with the first one using fuming nitric acid to attack any exposed Cu metal, and the second one using NaOH to remove the Al cap and the barrier to reveal the passivation layer underneath the POP location. Each POP bond pad is examined with high magnification optical microscope at 500X, for passivation cracking or copper line corrosion.

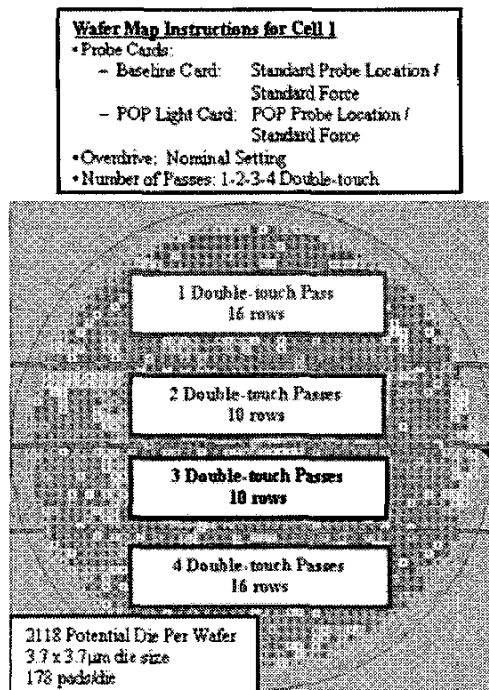


Figure 6: Wafer Map Instruction for Cell 1

b) Wire Bond Yield

Since the intent of the POP concept is to minimize non-stick-on-pad (NSOP) defect at wire bonding by eliminating the interaction between probing and wire bond processes, the

main assembly response presented in this paper will be the NSOP defect rate when wire bonding the test dice on a 160 I/O 15x15mm 1mm pitch PBGA. Although the wafers used in the probe experiments described in the previous section were probed at both the standard and POP locations, the wafers sent for assembly evaluation were probed only at the POP locations, leaving the standard probe location un-probed for wire bonding. The targeted ball bond diameter was 40 μ m using 20 μ m Au wire. The NSOP rate for the test vehicle using POP bond pads was compared with NSOP rate observed in production devices wire bonded with similar ball bond diameters on production probe marks. The expectation was that the NSOP rate for the POP bond pads would be substantially lower than that of production devices.

c) Product and Package Reliability Testing

The test dice were submitted to standard device and package qualification testing. Device-related testing included Dynamic High Temperature Operating Life (HTOL) (125°C with dynamic bias for a minimum of 168 hours), Static Bake (150°C for a minimum of 168 hours), ESD Human Body Model (2000V requirement) and Machine Model (200V requirement), and Latch-up (200mA requirement). Package-level reliability testing was performed on the packages, which began with Moisture Sensitivity Level 3 (MSL3) preconditioning (10 cycles of temperature cycling at -65°C to 150°C, bake at 125°C/24hours, moisture soak at 30°C, 60%RH for 192 hours, and 3 cycles of forced convection reflow at 220°C). After MSL3 preconditioning, parts were split and subjected to Air-to-Air Temperature Cycling (-65°C to 150°C for 100 cycles), Autoclave (121°C, 100%RH, 15PSIG for 48 hours), and Temperature-Humidity-Bias THB (85°C, 85%RH, bias for 500 hours).

There are two failure mechanisms of primary concern: (1) electrical performance after stress testing; and (2) delamination of the extended aluminum cap bond pads to the mold compound.

Results

a) Probe Performance Comparison between Standard Probe Location and POP Location:

The probe yield comparison among Baseline and POP Light cards is summarized in Table 3. For Wafer 1, the overdrive setting was the same for both probe cards. For Wafer 2, the overdrive for the Baseline probe card was set 20% higher than the overdrive of the POP Light card. In both cases, since the wafers and test program were still at an early development stage, only subtle differences in probe yield could be seen. However, the results were adequate enough to indicate no probe yield degradation due to probing on the POP location. As expected, the results for Wafer 2 indicate that there is a slight advantage of increasing the overdrive setting to produce better contact between the pad and probe needle.

Table 3: Probe Yield Comparison between Baseline and POP Light Probe Cards

| Wafer ID | # of Passes | Baseline Overdrive | POP Light Overdrive | Probe Yield Difference (POP Light – Baseline) |
|----------|-------------|--------------------|---------------------|---|
| 1 | 1 | N | N | 4.2 |
| | 2 | N | N | 1.4 |
| | 3 | N | N | 1.0 |
| | 4 | N | N | -1.2 |
| 2 | 1 | N+ | N | 0.0 |
| | 2 | N+ | N | -2.1 |
| | 3 | N+ | N | 0.0 |
| | 4 | N+ | N | -.05 |

Note: N denotes nominal probe card overdrive and N+ denoted the nominal value plus 20% for the overdrive set up

In Table 4, the probe yield comparison between Baseline and POP heavy cards is made. Results from wafer 3 suggest that increasing the overdrive setting may improve probe test yield, especially when only 1 pass is made at probe. However, similar to the results in Table 3, the differences are very small. Nevertheless, the results at least confirm the equivalency in probe yield from both standard and POP locations.

Table 4: Probe Yield Comparison between Baseline and POP Heavy Probe Cards

| Wafer ID | # of Passes | Baseline Overdrive | POP Heavy Overdrive | Probe Yield Difference (POP Heavy – Baseline) |
|----------|-------------|--------------------|---------------------|---|
| 3 | 1 | N | N+ | 8.6 |
| | 2 | N | N+ | -0.4 |
| | 3 | N | N+ | 0.2 |
| | 4 | N | N+ | 0.0 |
| 4 | 1 | N+ | N+ | -0.3 |
| | 2 | N+ | N+ | 1.0 |
| | 3 | N+ | N+ | 2.5 |
| | 4 | N+ | N+ | 0.2 |

Note: N denotes nominal probe card overdrive and N+ denoted the nominal value plus 20% for the overdrive set up

As mentioned in the Experimental Approach Section, the second objective in comparing probe performance was to ensure no passivation cracking or copper metal damage underneath the POP probe marks. Actual probe mark photographs captured microscopically are shown in Figure 7. The picture compares probe marks made by the Baseline card on the standard location and the POP Heavy card on the POP

location. Here, the larger and darker probe marks created by the POP heavy card with a higher spring force are clearly seen. The probe marks on the standard location are smaller and lighter. The bond pads in the picture underwent four probe passes.

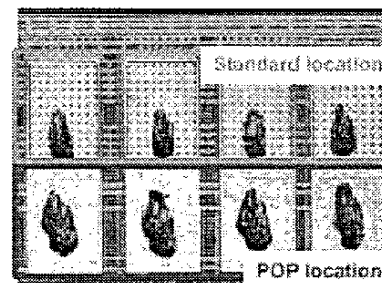


Figure 7: Probe Marks Generated by Baseline and POP Heavy Probe Cards

Figure 8 shows the standard and POP locations after the aluminum cap has been etched off in order to inspect for barrier layer damage. No damage could be found at either location.

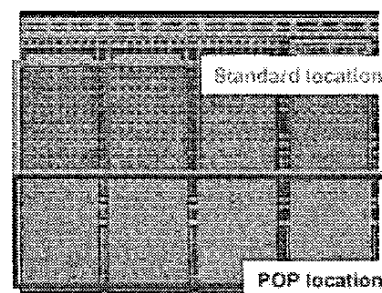


Figure 8: Barrier Layer after Al cap Removal

For the photograph shown in Figure 9, the barrier layer was removed to expose the underlying copper and passivation layer. The area of primary interest was the POP location, where no damage to the passivation layer was seen.

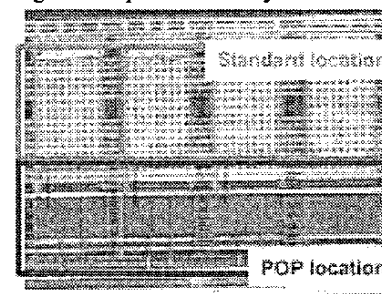


Figure 9: Copper and Passivation Layers after Al cap Removal

To further confirm that probing on the POP location did not damage the underlying passivation layer, cross sections of the bond pads were made with a FIB (Focused-Ion-Beam), then inspected via SEM. The SEM images are presented in Figure 10 – 12. From Figure 11, it was clearly seen that both the barrier and passivation layer underneath the POP aluminum cap region had no damage. In Figure 12, underneath the standard probe location, the barrier layer

between aluminum bonding area and copper layer also indicates no damage. However, the deepest part of the probe mark is very close to the top of the barrier layer. This means that any variations in the probe process may cause the barrier layer to be removed, exposing underlying copper. Therefore, although no damage is seen at the standard probe location, the possibility of having the probe marks scrub through the barrier and copper bond pad is very high.

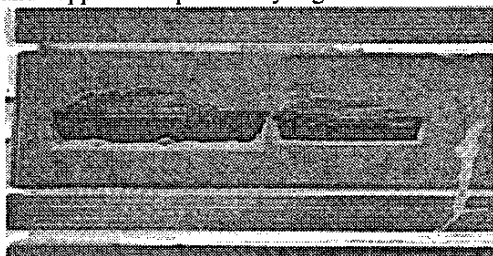


Figure 10: FIB Cross Section

Left: POP Location, Right: Standard Location

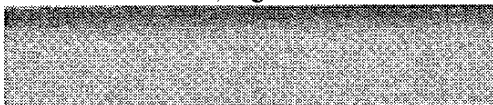


Figure 11: Close up of FIB Cross Section at POP location.



Figure 12: Close up of FIB Cross Section at Standard Location

Therefore, the results of visual inspection after etching, and FIB cross-sectioning verified that no mechanical damage was induced in the passivation layer underneath the POP location.

b) Wire Bond Yield:

The data in Table 5 demonstrates that as wire bond ball diameter decreases, the NSOP defect rate increases. This is largely due to the increase in probe mark and disturbed aluminum area to bonded ball diameter area ratio as bond diameter decreases. Assembling the test vehicle with probing performed on the POP location and leaving the standard location intact for wire bonding a 40 μ m ball bond diameter resulted in 0% NSOP due to probe mark. This improvement cannot be achieved by any type of parameter optimization at wire bonding.

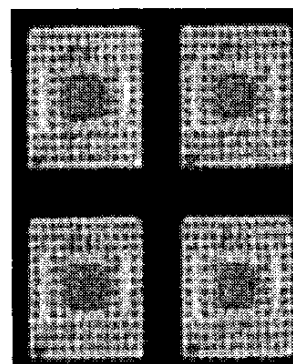
Table 5: NSOP% Comparison Among Devices with Different Bonded Ball Diameters

| Device Name | BBD (μ m) | NSOP Rejects/ Wire Bond Rejects |
|-----------------|----------------|------------------------------------|
| Device 1 | 60 | 41 % |
| Device 2 | 50 | 64 % |
| Device 3 | 35 | 84 % |
| Device with POP | 40 | 0% |

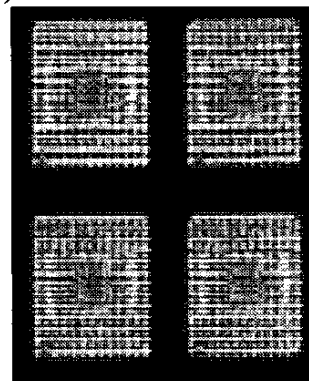
Note: Device 3 is a fine pitch wire bond test vehicle whose sample size is limited to an experimental scale

c) Reliability

Scanning Acoustic Microscopy (SAM) analysis before and after MSL3 preconditioning showed no delamination at the interface between the extended aluminum surfaces and the molding compound. Sample SAM images are shown in Figure 13.



(a) Before MSL3 Preconditioning



(b) After MSL3 Preconditioning

Figure 13: SAM Images Before and After MSL3 Preconditioning

Sample Size: 60 packages

Product qualification data for a device fabricated with POP is summarized in Table 6. The results demonstrate that introduction of the new POP pad did not cause package reliability issues.

Table 6: Product Qualification Results for Device with POP

| Stress Description | Testing/ Approval Done | Comments |
|--------------------|----------------------------|--|
| HTOL Dynamic | passed 168hrs | FITs \leq 250 |
| Static Bake | passed 168 hrs | 125C Ta; Tmax < materials capab. |
| HBM MM | passed 2kV HBM and 200V MM | |
| Latch-up | passed 200mA | |
| Temp. Cycling | passed 100 cycles | MSL3 preconditioning (-65 to 150 C); more cycles pending |
| Autoclave | passed 48 hrs | MSL3 preconditioning; more hours pending |
| THB | passed 500 hrs | 85°C/85%RH |

Note: Sample sizes are defined based on JEDEC and Motorola internal semiconductor product qualification requirements

Conclusions and Recommendations

The presence of an aluminum cap above the copper bond pad allows for extension of the cap without changing the bond pad size. This enables a long bond pad with separate probe and wire bond regions without incurring any additional cost or increase in die size.

Probe evaluations demonstrated equivalent electrical test yield between probing over the standard location as compared to the POP location. Mechanically, acid etching and FIB results confirmed no cracking in the passivation layer under the aluminum cap, even after four passes of double-touch probe at a heavy overdrive setting. With addition evaluations, it is possible that the probe test yield can be improved. This is because the probe needle spring force and probe overdrive setting can be increased without the concern of punching through the aluminum cap and exposing copper.

Wire bond yield data indicated that when the bonded ball diameter was 35 μ m, the ratio of NSOP due to probe mark to total wire bond rejects could be as high as 84%. By separating the probe and wire bond regions, a clean pad is available for bonding. For a device with a 40 μ m ball bond, there was zero NSOP due to probe mark damages after POP implementation.

Moisture characterization images of 60 units eradicated concerns of poor adhesion between the aluminum cap and the mold compound. POP was introduced into a new product. To date, all the product qualification stress tests indicate acceptable performance.

Acknowledgments

The authors would like to thank the following people for their support in their respective expert areas: Al Maus for POP pad design, Soosan Yong for handling assembly requirements, Chuck Miller for chemical etching, and Fonzell Martin, Marcus Fletcher, and Jeff Blackwell for new product introduction activities.

References

1. T. Tran, L. Yong, B. Williams, S. Chen and A. Chen "Fine Pitch Probing and Wirebonding and Reliability of Aluminum Capped Copper Bond Pads", Proceedings for 50th Electronic Components and Technology Conference, Las Vegas, Nevada, May 21-24, 2000.
2. T. Tran, L. Yong, B. Williams, S. Chen and A. Chen "Fine Pitch Probing and Wirebonding and Reliability of Aluminum Capped Copper Bond Pads", Proceedings for 2000 International Conference on High-Density Interconnect and Systems Packaging, IMAPS/ CMP, Denver, Colorado, April 26-28, 2000, pp. 390-395.
3. L. Mercado, R. Radke, M. Ruston, T. Tran, B. Williams, L. Yong, A. Chen and S. Chen, "Fine Pitch Probing and Wirebonding and Reliability of Multi Layer Copper Interconnect Structures", *Proc 33rd International Symposium on Microelectronics, IMAPS*, Boston, MA, September 2000, pp. 727-732.